

Correlation Analysis of Biological Effects of P53 Mutant Triple-Negative Breast Cancer with DCE-MRI Features

Jing Ren¹, Qiang Zhang^{2*}, Xiang Zhuang³

¹Baotou Medical College, Baotou 014040, China

^{2,3}Baotou Cancer Hospital, Baotou 014040, China

¹234244011@qq.com, ²hq-1234567@163.com

*Correspondence Author

Abstract: ***Objective:** To explore the correlation between the biological effects of P53 mutant and P53 wild-type in triple-negative breast cancer (TNBC) with dynamic contrast-enhanced magnetic resonance imaging (DCE-MRI) signs, semi-quantitative parameters, and quantitative parameters. **Methods:** A retrospective analysis was conducted on 68 patients diagnosed with TNBC at Baotou Cancer Hospital from December 2022 to August 2024, including 48 cases of P53 mutation and 20 cases of P53 wild-type. The differences between the two groups were compared in MRI signs including [lesion maximum diameter, apparent diffusion coefficient (ADC), lesion morphology, quantity, lymph node metastasis, intratumoral T2WI signal intensity, peritumoral edema, and early enhancement pattern], semi-quantitative parameters [signal enhancement ratio (SER), maximum enhancement rate (Epeak), time to peak (TTP), wash-in rate, wash-out rate, briefness of enhancement (BoE), and area under the curve (AUC)], and quantitative parameters [volume transfer constant (Ktrans), rate constant (Kep), and extracellular extravascular volume fraction (Ve)]. **Results:** Compared with TNBC-P53 wild-type, TNBC-P53 mutant showed differences in intratumoral T2WI high signal, early ring enhancement, Epeak, TTP, Ktrans, and Kep ($P < 0.05$), while there was no statistical difference between the two groups in patient age, menopausal status, lymph node metastasis, and MRI signs including maximum diameter, ADC value, morphological appearance, quantity, peritumoral edema, and semi-quantitative parameters SER, wash-in, wash-out, BoE, AUC, and quantitative parameter Ve ($P > 0.05$). A binary logistic regression model was used for analysis, and TTP and Ktrans were found to be more effective in determining mutation status. **Conclusion:** Intratumoral T2WI high signal, early ring enhancement, Epeak, TTP, Ktrans, and Kep are correlated with TNBC-P53 gene mutations.*

Keywords: Triple-negative breast cancer (TNBC), P53 gene, Dynamic contrast-enhanced magnetic resonance imaging (DCE-MRI), Semi-quantitative parameters, Quantitative parameters.

1. Introduction

Breast cancer has become one of the most prevalent cancers among women worldwide, with a high and persistent mortality rate [1]. In 2022, the incidence rate of breast cancer in China reached 11.5%, making it the most common malignant tumor domestically [2]. Breast cancer poses a significant threat to the life and health of women. According to the classification based on pathological immunohistochemical markers, when estrogen receptor (ER), progesterone receptor (PR), and human epidermal growth factor receptor 2 (HER2) are all negative or lowly expressed, it is referred to as triple-negative breast cancer (TNBC). Compared to other molecular subtypes, TNBC is characterized by an earlier age of onset, higher aggressiveness, poorer prognosis, and a higher risk of recurrence and metastasis [3], and it has limited response to chemotherapy, endocrine therapy, and targeted therapy drugs [4]. Therefore, it is particularly urgent to find more precise and effective treatment options for patients with TNBC.

P53 is a tumor suppressor gene that can induce apoptosis in cancer cells, prevent carcinogenesis, and assist in repairing defects in cellular genes. P53 mutations can promote tumor angiogenesis, increase tumor blood flow perfusion, providing more nutrients and oxygen for tumor growth; they can also evade immune system surveillance and attack through various mechanisms, promoting tumor metastasis. Literature reports that up to 80% of TNBC patients overexpress the P53 tumor suppressor protein (mutant form of the p53 tumor suppressor

protein, mtp53), and mutant P53 is expected to become a potential therapeutic target for TNBC [5-6]. Therefore, determining whether the P53 gene is mutated in TNBC patients is of significant clinical importance for developing personalized treatment plans and identifying potential effective targets for chemotherapy. Due to the low positive rate of P53 mutations in blood tests, the main method currently used to determine this is through immunohistochemical detection of biopsy or postoperative pathological samples, a method that is invasive and difficult to repeat. DCE-MRI, as a non-invasive examination, reduces patient pain and risk, and its repeatability allows for multiple imaging assessments of tumor changes during treatment. Its high soft tissue resolution also provides morphological and functional information about the lesion, aiding in more accurate identification of tumor characteristics [7]. DCE-MRI can also provide a variety of quantitative and semi-quantitative parameters that reflect the biological characteristics of tumor angiogenesis, vascular permeability, and microenvironment [8], offering strong evidence for indicating P53 mutations.

2. Study Subjects and Research Methods

2.1 Subjects of the Study

This study retrospectively analyzed patients who underwent breast DCE-MRI scans at Baotou Cancer Hospital from December 2022 to August 2024. A total of 68 cases were selected, all of which were confirmed as Triple-Negative

Breast Cancer (TNBC) by needle biopsy pathology and had not received any treatment. All patients underwent P53 gene mutation testing, and the results were divided into two groups: the experimental group consisted of 48 TNBC patients with P53 mutations, while the control group included 20 TNBC patients with wild-type P53. Clinical data included the patients' age and menopausal status. The age range of the patients was from 38 to 79 years, with an average age of 58.6 ± 8.9 years. Inclusion criteria were: 1) Pathologically diagnosed with TNBC; 2) Underwent dynamic contrast-enhanced examination on the same MRI scanner, and had not received surgery or chemotherapy before the examination; 3) Had P53 gene testing results; 4) Had complete clinical and DCE-MRI image data. Exclusion criteria were: 1) Non-TNBC patients; 2) Did not undergo P53 gene testing; 3) Patients had received relevant anti-tumor treatment before breast MRI examination; 4) Poor image quality, unable to accurately outline the region of interest.

2.2 Instruments and Inspection Methods

The bilateral breasts were scanned using the Philips Achieva 1.5T superconducting magnetic resonance imaging system and an 8-channel dedicated phased-array surface coil for breast imaging. During the examination, the subject was in a prone position with both breasts naturally hanging and placed within the scanning area. The scan included T1-weighted imaging (T1WI), T2-weighted imaging (T2WI), diffusion-weighted imaging (DWI), and other plain scan sequences, as well as the first phase sequence of dynamic contrast-enhanced magnetic resonance imaging (DCE-MRI). Gadopentetate dimeglumine at a rate of 2 mL/s in doses of 0.1–0.2 mmol/kg and 20 mL of saline were sequentially injected, and DCE-MRI images were continuously acquired, resulting in a total of 8 phases of images. The scanning parameters for the DCE-MRI sequence were: repetition time (TR) 6.9ms, echo time (TE) 3.4ms, matrix size 220×398 , slice thickness 1.2mm, with a total of 784 slices scanned, and the scanning time for each phase was 1 minute and 16.6 seconds.

2.3 Analysis of DCE-MRI Images and Measurement of Data

2.3.1 Image Processing

Collected and organized tumor signs in MRI images of each sequence by a chief radiologist and an associate chief physician. Selected cases for region of interest (ROI) delineation on the Philips post-processing workstation, choosing the area with the most significant early enhancement as the ROI for analysis, thereby obtaining ADC values, quantitative and semi-quantitative parameters. For disagreements in the analysis results, a consensus was reached through joint discussion.

2.3.2 MRI Sign Data Acquisition

Including the maximum diameter of the lesion, the apparent diffusion coefficient (ADC), lesion morphology (mass/non-mass), quantity (single/multiple), lymph node metastasis (yes/no), intratumoral T2WI signal intensity (high signal/equal signal) and surrounding edema (yes/no), early enhancement pattern (non-ring enhancement/ring enhancement).

2.3.3 Semi-quantitative Parameter Acquisition

In the enhanced image, select the layer with the most significant enhancement effect to outline the region of interest (ROI), thereby obtaining a series of semi-quantitative parameters, including: the relative enhancement rate (SER), the maximum enhancement rate (Epeak), the time to peak (TTP), the wash-in rate, the wash-out rate, the brevity of enhancement (BoE), and the area under the curve (AUC), see Figure 1. Absolute and relative maximum enhancement: the difference between the peak intensity and the baseline intensity (S_0); Time to peak (TTP): the time required from the first MRI sequence (T_0) to reach the peak intensity; Wash-in rate: the maximum slope between T_0 and the peak intensity time, which reflects the maximum rate of contrast agent uptake and can effectively evaluate the degree of early enhancement of tumor tissue; Wash-out rate: the absolute value of the maximum slope between the peak intensity time and the final measurement point, which determines the maximum rate of contrast agent outflow; Brevity of enhancement: the time difference between wash-in and wash-out; Area under the curve (AUC): the sum of the area under the contrast agent concentration-time curve (integral) [9].

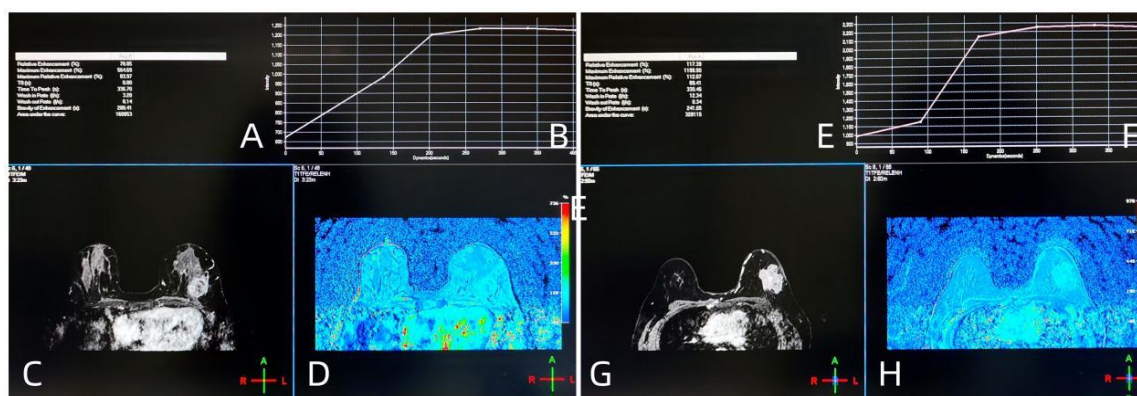


Figure 1: A-D represents TNBC-P53 mutant type; E-H represents TNBC-P53 non-mutant type
A, E: Semi-quantitative parameters; B, F: TIC curve shows a plateau type (II); C, G: Outline the area of strongest early enhancement as ROI; D, H: Quantitative parameter pseudo-color map

2.3.4 Acquisition of quantitative parameters

Using T2-weighted imaging (T2WI) as the reference image, select the level with the maximum signal abnormality on the dynamic enhanced image to draw a region of interest (ROI), avoiding areas such as cystic degeneration, calcification, and hemorrhage; based on the pharmacokinetic model, calculate the following quantitative parameters: Volume transfer constant (K_{trans}): the speed constant for the contrast agent to diffuse from the intravascular to the extravascular space; Rate constant (K_{ep}): the speed constant for the contrast agent to return from the interstitial space back into the vasculature; Extravascular extracellular volume fraction (V_e): the volume fraction of the extravascular extracellular space relative to the entire voxel; the units for these parameters are per minute (min⁻¹).

2.4 Statistical Methods

This study utilized SPSS 25.0 and Excel 2016 for data organization and analysis. For categorical data, the number of cases (percentage) was used for description, and independent samples t-test was applied to data conforming to normal distribution; for data that did not conform to normal distribution, median (interquartile range) was used, and Mann-Whitney U non-parametric rank-sum test was applied for analysis. Variables that were significant in univariate analysis were included in the binary logistics regression

model for in-depth analysis, and the variables significant in multivariate analysis were further evaluated using ROC curves, calculating sensitivity, specificity, Youden index, and cut-off values. In this research project, P<0.05 was used as the indicator for statistically significant differences.

3. Results

3.1 Comparison of General Data and MRI Features

In the cases of TNBC-P53 mutation type, 43 cases (89.6%) showed high signal intensity within the tumor on T2-weighted imaging (T2WI), and 38 cases (79.2%) exhibited ring enhancement in the early phase of magnetic resonance imaging dynamic contrast enhancement (MRI-DCE); in the cases of TNBC-P53 wild type, 13 cases (65.0%) showed high signal intensity within the tumor on T2WI, and 11 cases (55.0%) exhibited ring enhancement in the early phase of MRI-DCE, as seen in Figure 2. The differences in tumor internal T2WI signal intensity and early enhancement patterns between the two groups were statistically significant (P<0.05). No statistically significant differences were found between the two groups in terms of patient age, menopausal status, lymph node metastasis, as well as the maximum diameter, ADC value, morphology, number, and peritumoral edema in MRI features (P>0.05), as shown in Table 1.

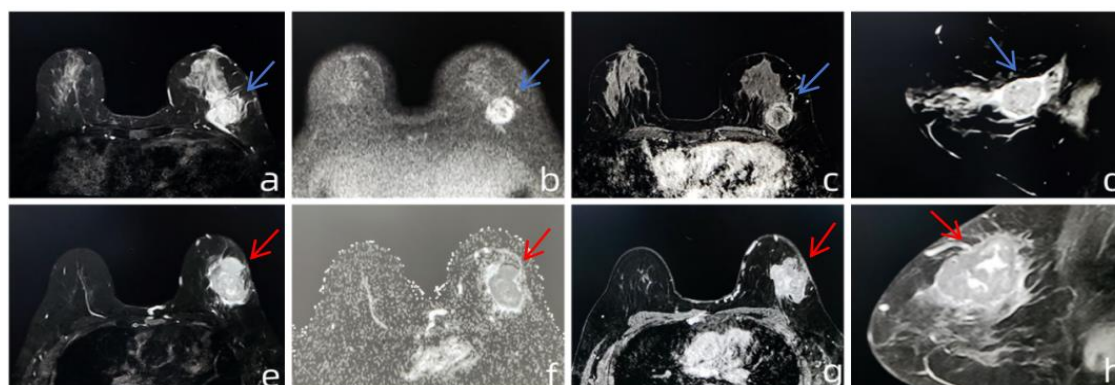


Figure 2: Typical MRI signs of TNBC-P53 mutation and wild-type patients

a-d: TNBC-P53 mutation type; e-h: TNBC-P53 wild type; a: Intra-tumoral high signal on T2WI (blue arrow); b: High signal on diffusion (blue arrow); c: Axial view: early enhancement showing ring-like enhancement (blue arrow); d: Sagittal view: early enhancement showing ring-like enhancement (blue arrow); e: Intra-tumoral isosignal on T2WI (red arrow); f: High signal at diffusion edge (red arrow); g: Axial view: early enhancement showing non-ring-like enhancement (red arrow); h: Sagittal view: early enhancement showing non-ring-like enhancement (red arrow)

Table 1: Comparison of general data and MRI signs between two groups

	Experimental group	Control group	t/χ^2	P
Age	59.15±9.43	58.75±7.99	0.165#	0.870
Menopausal status			0.108*	0.743
No	8(16.7)	4(20.0)		
Yes	40(83.3)	16(80.0)		
Lymph node metastasis			0.196*	0.658
No	12(25.0)	4(20.0)		
Yes	36(75.0)	16(80.0)		
Maximum diameter of the lesion	3.14±0.42	3.11±0.35	0.310#	0.758
Apparent Diffusion Coefficient (ADC)	0.86±0.03	0.85±0.01	1.150#	0.254
Lesion morphology			0.286*	0.593
Mass	43(89.6)	17(85.0)		
Non-mass	5(10.4)	3(15.0)		
Quantity			0.122*	0.727
Single	34(70.8)	15(75.0)		

	several	14(29.2)	5(25.0)		
Intratumoral T2WI signal intensity				5.871*	0.015
High signal		43(89.6)	13(65.0)		
Wait for the signal		5(10.4)	7(35.0)		
Peri-edema				0.426*	0.514
No		13(27.1)	7(35.0)		
Yes		35(72.9)	13(65.0)		
Reinforcement method				4.095*	0.043
Non-circular reinforcement		10(20.8)	9(45.0)		
Annular reinforcement		38(79.2)	11(55.0)		

Note: * indicates that the statistic is χ^2 , # indicates that the statistic is t.

3.2 Semi-quantitative Parameter Comparison

When comparing the experimental group with the control group, there was a statistically significant difference in the maximum enhancement rate and time to peak (P<0.05). The

experimental group had a higher maximum enhancement rate and a shorter time to peak compared to the control group, indicating that the maximum enhancement rate of TNBC-P53 mutant lesions is higher and the time to reach peak enhancement is faster. In the comparison of other indicators, there was no statistical difference between the two groups ($P>0.05$), as shown in Table 2.

Table 2: Two groups of DCE-MRI semi-quantitative parameters

	Experimental group	Control group	t	P
Relative enhancement	106.65±23.97	109.06±20.35	-0.394	0.695
Maximum enhancement	1215.44±255.45	835.20±195.98	5.957	0.000
Peak time	235.83±113.37	445.51±85.51	7.426	0.000
Washing rate	7.18±1.86	6.91±0.77	0.867	0.389
Rinse rate	0.91±0.56	0.85±0.44	0.378	0.706
Enhanced transiency	217.04±72.74	214.71±33.97	0.136	0.892
Area under the curve	292945.67±55161.71	298878.00±49098.17	-0.417	0.678

3.3 Results of Correlation Analysis

Binary logistic regression models were employed for analysis, with the occurrence of mutation as the dependent variable and four observation indicators selected as independent variables: intratumoral T2WI signal intensity, whether the lesion shows ring enhancement, maximum enhancement, and time to peak. The analysis results indicated that both maximum enhancement and time to peak are correlated with the occurrence of mutation ($P<0.05$). Time to peak is an independent risk factor for mutation ($OR<1$), while maximum enhancement rate serves as an independent protective factor ($OR>1$). Intratumoral T2WI signal intensity and whether the lesion shows ring enhancement did not show correlation as independent influencing factors with patient mutation ($P>0.05$), as shown in Table 3.

Table 3: Logistics of variables with differences between the two groups

	B	SE	Wald	df	P	OR (95%CI)
Intratumoral T2WI signal intensity	-2.818	2.426	1.349	1	0.245	0.060(0.001-6.936)
Intratumoral T2WI signal intensity	0.775	1.510	0.264	1	0.608	2.171(0.113-41.838)
Maximum enhancement	2.631	0.964	7.454	1	0.006	13.885(2.100-97.783)
Peak time	-4.248	3.295	6.326	1	0.012	0.014(0.001-0.392)

Compared with the control group, the experimental group performed better in terms of judging mutation efficacy with the ratio of peak time to maximum enhancement. When the sensitivity reached 0.972, the specificity was 0.688, and the Youden index was also 0.688, with the cut-off value set at 1100.00, the diagnostic index for peak time could reach as high as 0.913, as shown in Figure 3 and Table 4.

Table 4: AUC, Sensitivity, Specificity, Youden Index, and Cut-off Value of Risk Factors

	AUC	P	Sensitivity	Specificity	Youden Index	Truncation value
Maximum enhancement	0.877(0.796-0.958)	0.000	0.972	0.688	0.688	1100.00
Peak time	0.913(0.845-0.980)	0.000	0.950	0.790	0.742	333.9376

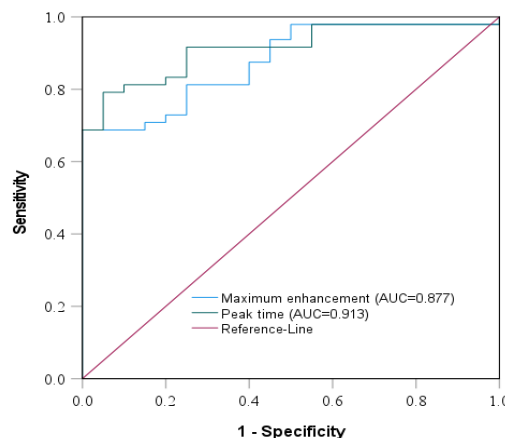


Figure 3: ROC Curve Analysis for Maximum Enhancement and Peak Time

3.4 Quantitative Parameter Comparison

The average values of K_{trms} , V_e , and K_{ep} for the experimental group were $(1.91±0.11) \text{ min}^{-1}$, $(0.80±0.09) \text{ min}^{-1}$, and $(2.42±0.31) \text{ min}^{-1}$, respectively; the corresponding values for the control group were $(1.71±0.10) \text{ min}^{-1}$, $(0.81±0.07) \text{ min}^{-1}$, and $(2.12±0.17) \text{ min}^{-1}$. Between the two groups, the differences in K_{trms} values and K_{ep} values were statistically significant ($P<0.05$), as shown in Table 5.

Table 5: Quantitative Parameters of Two Groups of DCE-MRI

	Experimental group	Control group	t	P
Volume transfer (K_{trms})	1.91±0.11	1.71±0.10	6.728	0.000
v_e	0.80±0.09	0.81±0.07	-0.528	0.600
Rate constant (K_{ep})	2.42±0.31	2.12±0.17	5.006	0.000

The K_{trms} value has shown high accuracy in assessing mutation efficacy, with a sensitivity of 0.650, a specificity of up to 0.950, a Youden index of 0.650, and when the cut-off value is set at 1.735, the diagnostic index can reach a maximum value of 0.888, as shown in Figure 4, Table 6.

Table 6: AUC, Sensitivity, Specificity, Youden Index, and Cutoff Value of DCE-MRI Quantitative Parameters

	AUC	P	Sensitivity	Specificity	Youden Index	Truncation value
Volume transfer (K_{trms})	0.888(0.804-0.973)	0.000	0.650	0.950	0.650	1.735
Rate constant (K_{ep})	0.798(0.693-0.903)	0.000	0.800	0.688	0.538	2.257

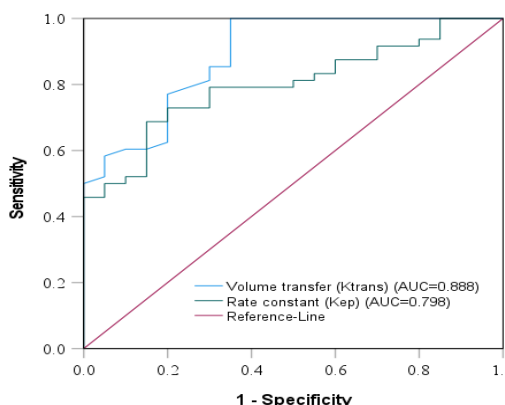


Figure 4: ROC curve for volume transfer and rate constant

4. Discussion

TNBC is a highly invasive and heterogeneous subtype of breast cancer characterized by the absence of expression of estrogen receptors (ER), progesterone receptors (PR), and human epidermal growth factor receptor 2 (HER2), which leads to its poor responsiveness to endocrine therapy and targeted therapy [10]. Currently, chemotherapy remains the primary treatment strategy for triple-negative breast cancer, but its efficacy is limited and it has certain adverse effects. Although emerging treatment modalities such as immunotherapy and targeted therapy are being actively researched, they have not yet become widely recognized standard treatment protocols [11]. P53 gene mutations play an important clinical and biological role in TNBC, and mutations in this gene result in the loss of tumor suppressor function, allowing tumor cells to evade cell death mechanisms and accelerate tumor progression. In patients with triple-negative breast cancer, the mutation rate of the P53 gene is as high as 80% [12]. P53 gene mutations further complicate the treatment of triple-negative breast cancer (TNBC), as these mutations may cause tumor cells to develop resistance to chemotherapy drugs [13]. Therefore, the early identification of P53 mutation status in TNBC is of significant clinical importance for clinicians to accurately assess patient prognosis, develop more individualized treatment plans, and prolong patient survival [13-15].

DCE-MRI can provide comprehensive information about lesions, including morphology, hemodynamic characteristics, and the tumor microenvironment. These data are helpful for a more comprehensive assessment of lesion characteristics and can non-invasively predict the molecular subtypes of breast cancer before surgery, avoiding invasive procedures, reducing patient pain and risk, and also providing important references for clinical decision-making and prognosis evaluation [16].

This study reveals that there is a correlation between TNBC-P53 gene mutations and tumor internal T2-weighted imaging (T2WI) signal intensity, ring enhancement phenomenon, Epeak value, TTP value, Ktrans value, and Kep value.

In lesions with TNBC-P53 gene mutations, 89.6% showed high signal on T2-weighted imaging (T2WI), while 79.2% presented ring enhancement in the early dynamic enhancement phase. After TNBC-P53 gene mutation, uncontrolled tumor growth leads to insufficient internal blood supply, which is prone to liquefaction necrosis. Due to the high water content in necrotic tissue, high signal is presented on T2WI. The reduction in cell components and perfusion in the necrotic area makes it difficult for contrast agents to enter, thus appearing as low or no enhancement areas on DCE-MRI. The increased active cell areas and new blood vessels at the tumor margin cause increased uptake of contrast agents, forming ring enhancement [17-20]. The ring enhancement in the early dynamic enhancement phase and the high signal sign of tumor internal T2WI indicate that the experimental group is more likely to develop tumor neovascularization and intratumoral necrosis compared to the control group, which is consistent with previous literature reports [21].

DCE-MRI can non-invasively reveal changes in tumor

microvasculature, comprehensively reflecting the perfusion status, vascular permeability, and extravascular (extracellular) space conditions of tumor tissues through TIC curves [22]. Its semi-quantitative parameters show significant correlation with tumor microvessel density and vascular endothelial growth factor [23-24], further revealing changes in tumor blood flow perfusion; the experimental group has higher Epeak values and shorter TTP, indicating a higher degree of tumor maximum enhancement, faster contrast agent reaching peak, meaning increased tumor neovascularization, sufficient blood supply, active angiogenesis, and increased perfusion [25-26]. Abundant vascular perfusion is associated with high invasiveness and rapid growth of tumors, also indicating a higher risk of tumor metastasis [27]. P53 mutations can also induce the expression of epithelial-mesenchymal transition (EMT)-related genes, such as Twist, ZEB-1, and ZEB-2, inhibit the expression of epithelial markers E-cadherin, thereby endowing tumor cells with stronger migratory and invasive capabilities, also indicating that tumors are more likely to metastasize to other sites through the blood or lymphatic system after P53 mutation, forming distant metastases [28].

DCE-MRI can quantify tumor perfusion, permeability, and the volume of the extravascular extracellular space by constructing pharmacokinetic models. The three commonly used quantitative parameters in this model include the volume transfer constant (Ktrans), the volume fraction of the extravascular extracellular space (ve), and the rate constant (kep) [29]. Ktrans represents the speed at which the contrast agent diffuses from the intravascular to the extravascular space, reflecting the transport rate from plasma to tissue, as well as the density and blood flow conditions of the newly formed microvessels in the tumor tissue. Based on the characteristics of tumor microvasculature, Ktrans can be used to assess tumor progression and may guide the formulation of subsequent treatment plans [30]. In this study, the Ktrans values of the experimental group were higher than those of the control group, indicating that the mutant tumors have richer vasculature and more vigorous blood flow. Kep is the reflux rate of the contrast agent, reflecting the ability of the contrast agent to return to the vascular space after diffusion, and it is generally considered to reflect the permeability of the microvasculature at the lesion site [31]. The Kep values of the experimental group were higher than those of the control group, suggesting that the permeability of the mutant tumor vasculature is greater. This further confirms that the rapid proliferation of tumor cells after P53 gene mutation leads to the accumulation of metabolic products within the tumor, which may increase the acidity of the local tissue environment, affecting the permeability of the vasculature, thereby affecting the outflow rate of the contrast agent.

Based on the comprehensive analysis, our research team has found differences between TNBC-P53 mutation type and wild type in tumor internal T2-weighted imaging (T2WI) signal intensity, ring enhancement phenomenon, Epeak, TTP, Ktrans, and Kep. In particular, TTP and Ktrans have shown high diagnostic efficacy, with their indication of genetic mutations being more significant, which helps provide a basis for clinical personalized treatment plans.

Our study also has certain limitations. Firstly, the sample size

of this study is relatively small, which may affect the efficacy of statistical analysis. Secondly, there are many human factors in the process of delineating the region of interest, which may affect the accuracy of the results to some extent. Future research will be dedicated to expanding the sample size and optimizing measurement methods, in the hope of obtaining more precise and reliable research results.

References

- [1] Bray F, Laversanne M, Sung H, Ferlay J, Siegel RL, Soerjomataram I, Jemal A. Global cancer statistics 2022: GLOBOCAN estimates of incidence and mortality worldwide for 36 cancers in 185 countries. *CA Cancer J Clin.* 2024 May-Jun;74(3):229-263. doi: 10.3322/caac.21834. Epub 2024 Apr 4. PMID: 38572751.
- [2] Ji YT, Liu SW, Zhang YM, Duan HY, Liu XM, Feng ZW, Li JJ, Lyu ZY, Huang YB. [Comparison of the latest cancer statistics, cancer epidemic trends and determinants between China and the United States]. *Zhonghua Zhong Liu Za Zhi.* 2024 Jul 23;46(7):646-656. Chinese. doi: 10.3760/cma.j.cn112152-20240208-00068. PMID: 38764329.
- [3] JIANG Y Z, MA D, SUO C, et al. Genomic and transcriptomic landscape of triple-negative breast cancers: subtypes and treatment strategies[J]. *Cancer Cell*, 2019, 35(3): 428-440. e5.
- [4] Xiao Hui, Zou Dan, Song Ailin. Advances in Targeted Therapy for Triple-Negative Breast Cancer [J]. *Chinese Journal of Endocrine Surgery*, 2022, 16(2):241-243. DOI:10.3760/cma.j.cn.115807-20210702-00205.
- [5] Wang Wenhui. The Effect of TYK2 and Mutant P53 on the Biological Behavior of Breast Cancer MDA-MB-231 Cell Line [D]. Dalian Medical University, 2017.
- [6] Xu Lisheng, Wang Shui, Zhao Zhihong, et al. Expression and Prognostic Study of VEGF and p53 in Tissue and Serum of Patients with Triple-Negative Breast Cancer [J]. *Journal of Nanjing Medical University (Natural Science Edition)*, 2021, 41(1): 118-121. DOI: 10.7655/NYDXBNS20210122.
- [7] Advances in Dynamic Contrast-Enhanced Magnetic Resonance Imaging for Predicting Breast Cancer Prognosis J. *Journal of Biomedical Engineering*, 2024, 37(1): 1-12. DOI: 10.12677/acm.2024.141134
- [8] Research Progress on the Diagnostic Value of DCE-MRI Combined with DWI in Breast Cancer J. *Advances in Clinical Medicine*, 2024, 14(1): 943-950. DOI: 10.12677/acm.2024.141134
- [9] Wang L, Van den Bos IC, Hussain SM, Pattynama PM, VogelMW, Krestin GP (2008) Post-processing of dynamic gadolinium-enhanced magnetic resonance imaging exams of the liver: explanation and potential clinical applications for color-coded qualitative and quantitative analysis. *Acta Radiol* 49(1):6-18
- [10] Dent R, Trudeau M, Pritchard KI, Hanna WM, Kahn HK, Sawka CA, Lickley LA, Rawlinson E, Sun P, Narod SA. Triple-negative breast cancer: clinical features and patterns of recurrence. *Clin Cancer Res.* 2007 Aug 1; 13(15 Pt 1): 4429-34. doi: 10.1158/1078-0432.CCR-06-3045. PMID: 17671126.
- [11] Zhao Wenkang, Zhang Jian. Research Progress in the Treatment of Triple-Negative Breast Cancer J. *Clinical Medical Progress*, 2024, 14(5): 362-368. DOI: 10.12677/acm.2024.1451435
- [12] Zhou Junzhen, et al. Research progress on mutant p53 as a potential therapeutic target for breast cancer. *J. Clinical Medical Progress*, 2021, 11(11): 5457-5460. DOI: 10.12677/acm.2021.1111807
- [13] Qin Zhang, Liu Hong. Expression and Clinical Significance of P53 in Triple-Negative Breast Cancer J. *Chinese Clinical Oncology*, 2011, 38(4): 161-164. DOI: 10.3969/j.issn.1000-8179.2011.04.010
- [14] Zhu Xiang. Research Progress on p53 Gene and Tumors J. *World Cancer Research*, 2022, 12(3): 152-160. DOI: 10.12677/wjcr.2022.123020
- [15] Cynthia X. Ma, et al. Targeting Chk1 in p53-deficient triple-negative breast cancer is therapeutically beneficial in human-in-mouse tumor models J. *The Journal of Clinical Investigation*, 2012, 122(4): 1398-1405. DOI: 10.1172/JCI58765
- [16] Dai Ting, Su Tong, Wang Rui, et al. Predictive value of DCE-MRI imaging features for hormone receptors, HER-2, and triple-negative breast cancer in breast cancer. *J. Magnetic Resonance Imaging*, 2023, 14(4): 57-67. DOI:10.12015/issn.1674-8034.2023.04.011
- [17] Current Status and Prospects of Research on Ring-Enhancing Lesions in Breast DCE-MRI. *J. Magnetic Resonance Imaging*, 2022, 13(2): 135-146. DOI: 10.12015/issn.1674-8034.2022.02.001
- [18] Du Hua. The role and mechanism of p53 in regulating cell cycle arrest and apoptosis. *J. International Journal of Radiation Medicine and Nuclear Medicine*, 2002, 26(2): 79-83. DOI: 10.16335/j.cnki.issn.1000-4655. 2002.02.013
- [19] LEEK RD, LANDERS RJ, HARRIS AL, et al. Necrosis correlates with high vascular density and focal macrophage infiltration in invasive carcinoma of the breast[J]. *Br J Cancer*,1999,79 (5 / 6):991.
- [20] Kato, F., Kudo, K., Yamashita, H., & Nishimura, T. (2016). MR imaging findings of triple-negative breast cancer: a pictorial essay. *Japanese journal of radiology*, 34(1), 1-9.
- [21] Correlation Study of p53 and Ki67 Expression in Triple-Negative Breast Cancer J. *Journal of Shanghai Jiaotong University (Medical Science)*, 2013, 33(6): 811-815. DOI: 10.3969/j.issn.1674-8115.2013.06.027
- [22] WU M,LU L,ZHANG Q,et al. Relating doses of contrast agent administered to TIC and semi quantitative parameters on DCE-MRI: based on a murine breast tumor model [J]. *PLoS One*, 2016,11(2):e0149279.
- [23] Wang Li, Zhai Renyou, Liu Xiaojuan, et al. Correlation between semi-quantitative parameters of dynamic contrast-enhanced breast MRI and vascular endothelial growth factor expression [J]. *Journal of Practical Radiology*, 2008, 24(7):946.
- [24] Wang Li, Zhai Renyou, Jiang Tao, et al. Correlation between dynamic enhanced MRI semi-quantitative parameters and microvessel density in breast diseases [J]. *Chinese Journal of Medical Imaging Technology*, 2007, 23(3):388.
- [25] Diagnostic Value of Breast MRI Signs and Semi-quantitative Enhancement in Triple-negative Breast Cancer J. *Journal of Bengbu Medical College*, 2023, 48(8): 1035-1039. DOI: 10.13898/j.cnki.issn.1000-2200.2023.08.018

- [26] Nian Z, Dou Y, Shen Y, Liu J, Du X, Jiang Y, Zhou Y, Fu B, Sun R, Zheng X, Tian Z, Wei H. Interleukin-34-orchestrated tumor-associated macrophage reprogramming is required for tumor immune escape driven by p53 inactivation. *Immunity*. 2024 Oct 8;57(10):2344-2361.e7. doi: 10.1016/j.immuni.2024.08.015. Epub 2024 Sep 24. PMID: 39321806.
- [27] Correlation Analysis of Breast Cancer DCE-MRI Parameters and ADC with Pathological Molecular Prognostic Markers *J. Magnetic Resonance Imaging*, 2021, 12(3): 283-288. DOI: 10.12015/issn.1674-8034.2021.03.001
- [28] Liu Y, Su Z, Tavana O, Gu W. Understanding the complexity of p53 in a new era of tumor suppression. *Cancer Cell*. 2024 Jun 10;42(6):946-967. doi: 10.1016/j.ccell.2024.04.009. Epub 2024 May 9. PMID: 38729160; PMCID: PMC11190820.
- [29] Wei Ling, Jiang Lin, Ma Xuejin, et al. Research Progress of Quantitative MRI in the Diagnosis of Breast Cancer [J]. *International Journal of Medical Radiology*, 2023, 46(01): 55-59. DOI:10.19300/j.2023.z20042.
- [30] Yu Jinfen, Wang Linsheng, Li Chuan Ting, et al. Clinical Value of MR DCE Ktrans Values in Laryngeal Cartilage Lesions [J]. *Chinese Journal of Medical Imaging*, 2022, 28(05): 466-471. DOI:10.19627/j.cnki.cn31-1700/th.2022.05.008.
- [31] Rao Deli, Qiu Xiaoming, Zhu Yanli. Observational Study on the Application of DCE-MRI Quantitative Parameters in the Staging and Prognostic Evaluation of Breast Cancer [J]. *Chinese Journal of CT and MRI*, 2024, 22(04): 89-91.